Non-Paraxial Split-Step Finite-Difference Method for Beam Propagation

Anurag Sharma and Arti Agrawal

Physics Department, Indian Institute of Technology Delhi, New Delhi 110016, India

Email: asharma@physics.iitd.ac.in

Abstract

A method based on symmetrized splitting of the propagation operator in the finite difference scheme for non-paraxial beam propagation is presented. The formulation allows the solution of the second order scalar wave equation without having to make the slowly varying envelope and one-way propagation approximations. The method is highly accurate and numerically efficient. Unlike most Padé approximant based methods, it is non-iterative in nature and requires less computation. The method can be used for bi-directional propagation as well.

1 Introduction

Modeling of practical guided-wave devices requires solution of the wave equation in a structure that may have complicated refractive index distribution and/or several branches. In most such structures, the paraxial approximation for beam propagation is not valid and its use may lead to large error in simulations. Thus, non-paraxial solutions are required. Several schemes have been suggested for wide-angle beam propagation through guided-wave devices (Yevick and Glasner, 1990; Hadley, 1992; Yamauchi et al., 1996; Ilić et al., 1996; Shibayama et al.; 1999, Ho and Lu, 2001; Lu and Ho, 2002; Lu and Wei, 2002; Luo and Law, 2002). Most methods for non-paraxial beam propagation discussed in the literature approach this problem iteratively, in which a numerical effort equivalent to solving the paraxial equation several times is involved. Most of these methods neglect the backward propagating components and solve the one-way wave equation. In these methods, the square root of the propagation operator involved in the wave equation is approximated in various ways. One of the approximations used is based on the Padé approximants (Yevick and Glasner, 1990; Hadley, 1992). Earlier, we proposed a new method (Sharma and Agrawal, 2004) based on symmetrized splitting of the operator for non-paraxial propagation using the collocation method (Sharma and Banerjee, 1989; Sharma, 1995). Recently, we have shown that the split-step non-paraxial scheme can be efficiently implemented in the finite-difference based propagation method (Sharma and Agrawal, 2005,

2006). In this paper, we describe the method in detail giving a comprehensive computational scheme and a detailed comparison with the collocation based split-step method and the Padé approximants based finite-difference methods.

2 Formulation

2.1 Split-Step Non-Paraxial Propagation (SSNP) Method

We consider, for simplicity, two-dimensional propagation; the scalar wave equation is then given by

$$\frac{\partial^2 \psi}{\partial x^2} + \frac{\partial^2 \psi}{\partial z^2} + k_0^2 n^2(x,z)\,\psi(x,z) = 0\,. \tag{1}$$

where $\psi(x,z)$ represents one of the Cartesian components of the electric field (generally referred to as the scalar field) and $n^2(x,z)$ defines the refractive index distribution of the medium. The time dependence of the field has been assumed to be $\exp(i\omega t)$ and $k_0 = \omega/c$ is the free space wave number. We write Eq.(1) as

$$\frac{\partial \mathbf{\Phi}}{\partial z} = \mathbf{H}(z)\,\mathbf{\Phi}(z)\,, \tag{2}$$

where

$$\mathbf{\Phi}(z) = \begin{bmatrix} \psi \\ \dfrac{\partial \psi}{\partial z} \end{bmatrix} \quad \text{and} \quad \mathbf{H}(z) = \begin{bmatrix} 0 & 1 \\ -\dfrac{\partial^2}{\partial x^2} - k_0^2 n^2 & 0 \end{bmatrix}. \tag{3}$$

The operator **H** can be written as a sum of two operators, one representing the propagation through a uniform medium of index, say n_r, and the other representing the effect of the index variation of the guiding structure; thus,

$$\mathbf{H}(z) = \begin{bmatrix} 0 & 1 \\ -\dfrac{\partial^2}{\partial x^2} - k_0^2 n_r^2 & 0 \end{bmatrix} + \begin{bmatrix} 0 & 0 \\ k_0^2 (n_r^2 - n^2) & 0 \end{bmatrix} \equiv \mathbf{H}_1 + \mathbf{H}_2(z) \tag{4}$$

A formal solution of Eq. (2) after symmetrized splitting of operators can be written as (Sharma and Agrawal, 2004, 2006)

$$\mathbf{\Phi}(z+\Delta z) = \mathbf{P}\,\mathbf{Q}(z)\,\mathbf{P}\,\mathbf{\Phi}(z) + O\left((\Delta z)^3\right) \tag{5}$$

where $\mathbf{P} = \mathrm{e}^{\frac{1}{2}\mathbf{H}_1 \Delta z}$ and $\mathbf{Q}(z) = \mathrm{e}^{\mathbf{H}_2 \Delta z}$. The operator $\mathbf{P}$ represents propagation in the uniform medium n_r over a distance of $\Delta z/2$, and hence, can be evaluated using any method like the collocation, finite-difference or FFT methods. The concept of splitting of operators is independent of the scheme used for propagation. The evaluation of $\mathbf{Q}(z)$ can be easily done due to the special form of the matrix $\mathbf{H}_2(z)$ as we shall see in the next subsection.

2.2 Finite-Difference Implementation of the SSNP Method

In this paper, we use the finite difference scheme to implement the SSNP method. In the finite-difference scheme, we have a set of $\psi_j(z) \equiv \psi(x_j, z);\ j = 1,2,\cdots,N_x$ specifying the field at different nodes x_j, at which the refractive index is defined as $n_j^2(z) \equiv n^2(x_j, z)$. We shall use the column vector $\boldsymbol{\psi}(z)$ to represent the field with $\psi_j(z)$ as its elements. The operator $\mathbf{Q}(z)$ can be easily evaluated due to the specific form of the matrix and it can be seen that

$$\mathbf{Q}(z) = \Delta z \begin{bmatrix} \mathbf{I} & \mathbf{0} \\ -k_0^2\,\mathbf{R}(z) & \mathbf{I} \end{bmatrix}, \tag{6}$$

since $[\mathbf{H}_2(z)]^m = 0$ for $m \geq 2$ due to the form of $\mathbf{H}_2(z)$. Here $\mathbf{R}(z)$ is a diagonal matrix with $R_{jj}(z) = n_j^2(z) - n_r^2$ as the diagonal elements. The evaluation of $\mathbf{P}$, on the other hand, amounts to solving the wave equation, Eq. (1), for a medium with a constant refractive index, n_r. Thus, we obtain (Sharma and Agrawal, 2004)

$$\mathbf{P} = \mathrm{e}^{\frac{1}{2}\mathbf{H}_1 \Delta z} = \exp\left\{ \frac{\Delta z}{2} \begin{bmatrix} \mathbf{0} & \mathbf{I} \\ -(\mathbf{S}_0 + k_0^2 n_r^2 \mathbf{I}) & \mathbf{0} \end{bmatrix} \right\} = \begin{pmatrix} \cos(\sqrt{\mathbf{S}}\,\Delta z/2) & \sin(\sqrt{\mathbf{S}}\,\Delta z/2)/\sqrt{\mathbf{S}} \\ -\sqrt{\mathbf{S}}\sin(\sqrt{\mathbf{S}}\,\Delta z/2) & \cos(\sqrt{\mathbf{S}}\,\Delta z/2) \end{pmatrix} \tag{7}$$

where $\mathbf{I}$ and $\mathbf{0}$ are the unit and null matrices, respectively, the operator $\mathbf{S} = \mathbf{S}_0 + k_0^2 n_r^2 \mathbf{I}$ and $\mathbf{S}_0$, in the present case, is a finite-difference representation of $\partial^2/\partial x^2$. The operator $\mathbf{P}$ represents propagation in uniform medium of index n_r over a distance of $\Delta z/2$. It is thus a constant square matrix and needs to be evaluated only once.

Next we consider the finite-difference representation of the $\partial^2/\partial x^2$. The differential term can be written as (see, *e.g.*, Khabaza, 1965)

$$\frac{\partial^2}{\partial x^2} = \frac{1}{\Delta x^2}\left(\delta_x^2 - \frac{1}{12}\delta_x^4 + \frac{1}{90}\delta_x^6 \cdots\right) \equiv \frac{1}{\Delta x^2}\left[2\sinh^{-1}\left(\frac{\delta_x}{2} \right) \right]^2 \tag{8}$$

where $\delta_x^2 \psi_p = \psi_{p+1} - 2\psi_p + \psi_{p-1}$ in the central difference scheme, and the δ_x^2 operator can be represented by a tri-diagonal matrix:

$$\delta_x^2 = \begin{bmatrix} -2 & 1 & 0 & \cdots & 0 \\ 1 & -2 & 1 & \cdots & 0 \\ 0 & 1 & -2 & \cdots & 0 \\ \vdots & \vdots & \vdots & \ddots & 1 \\ 0 & 0 & 0 & 1 & -2 \end{bmatrix} \equiv \mathbf{D}_x \tag{9}$$

By defining the δ_x^2 operator by the tri-diagonal matrix above, the series representing the transverse operator can be evaluated explicitly. Using the series expansion on the R.H.S. of Eq. (8) we obtain

$$\Delta x^2 \frac{\partial^2}{\partial x^2} = \left[2\sinh^{-1}\left(\frac{\delta_x}{2} \right) \right]^2 = 4\sum_{M=1}^{\infty} \left(\sum_{m=1}^{M} a_m a_{M-m+1} \right) \left(\frac{\delta_x^2}{4} \right)^M = \sum_{M=1}^{\infty} b_M (\delta_x^2)^M \tag{10}$$

where

$$\begin{aligned} b_M &= \frac{1}{4^{M-1}} \sum_{m=1}^{M} a_m a_{M-m+1} \\ a_{m+1} &= -\frac{(2m-1)^2}{2m(2m+1)} a_m, \quad a_1 = 1 \end{aligned} \tag{11}$$

Using the matrix form for δ_x^2 from Eq. (9) and the expansion from Eq. (10), we obtain

$$\mathbf{S} = k_o^2 n_r^2 \mathbf{I} + \frac{1}{\Delta x^2} \sum_{M=1}^{\infty} b_M \mathbf{D}_x^M = k_o^2 n_r^2 \mathbf{I} + \frac{1}{\Delta x^2} \left(\mathbf{D}_x - \frac{1}{12} \mathbf{D}_x^2 + \frac{1}{90} \mathbf{D}_x^3 - \frac{1}{560} \mathbf{D}_x^4 + \ldots \right) \tag{12}$$

Use of the first term (order, $M = 1$) in the series given by Eq. (12), corresponds to the approximation made in the Crank-Nicholson scheme (truncation error of Δx^2) and the first two terms (order, $M = 2$), to that in the Generalised Douglas (GD) scheme (truncation error of Δx^4, see, e.g., Sun and Yip, 1993). As the number of terms in the series expansion is increased, the matrix representation for the transverse derivative becomes denser and no longer remains tri-diagonal, however, the accuracy of $\partial^2 / \partial x^2$ increases. In the GD scheme based implicit *p*-step methods (Yamauchi et al., 1996; Shibayama et al., 1999), each propagation step is divided into *p* substeps and in each substep a system of N_x linear equations is solved. By truncating the series for the transverse derivative at the Δx^4 term, the matrix for the system of equation remains tri-diagonal and the efficient Thomas algorithm (Conte and deBoor, 1972) can be used for its solution. However, retaining higher order terms in the series expansion of the transverse derivative causes the system to have a matrix which has a bandwidth larger than three and the Thomas algorithm can no longer be used; this makes the method computationally inefficient.

Therefore, to retain computational efficiency, these methods neglect higher order terms. However, in the split-step method, the increase in matrix density does not alter the computation speed or efficiency significantly as only matrix multiplications are involved.

Physically, increasing the number of terms in the series in Eq. (12) corresponds to an increase in the number of nodal points which are involved in approximating $\partial^2/\partial x^2$, leading to a better representation of the derivative with respect to x, without having to adopt an iterative, multi-step procedure required in the conventional Padé analysis. Further since the evaluation of $\mathbf{P}$ has to be done only once, the increase in number of terms in the series expansion leads only to increase in the one time computation of $\mathbf{P}$ and does not noticeably increase the per-propagation-step computation time. This we have demonstrated in the next section.

2.3 Computation Scheme

The propagation method described by Eq.(5) is implemented as follows:

$$\mathbf{\Phi}(z+N_z\Delta z)=\mathbf{P}\,\mathbf{Q}(z+\{N_Z-1\}\Delta z)\,\mathbf{P}^2\,\mathbf{Q}(z+\{N_Z-2\}\Delta z)\cdots\cdots\mathbf{P}^2\,\mathbf{Q}(z+\Delta z)\,\mathbf{P}^2\,\mathbf{Q}(z)\,\mathbf{P}\,\mathbf{\Phi}(z) \quad (13)$$

where N_z is the number of propagation steps. In the above equation, $\mathbf{P}^2=\mathbf{PP}$ can be computed along with $\mathbf{P}$ and stored for subsequent use to reduce the computational effort. Since $\mathbf{P}$ is a 2×2 block matrix with each block being an $N_x\times N_x$ matrix, we can write it as

$$\mathbf{P}=\begin{pmatrix}\cos(\sqrt{\mathbf{S}}\,\Delta z/2) & \sin(\sqrt{\mathbf{S}}\,\Delta z/2)/\sqrt{\mathbf{S}}\\ -\sqrt{\mathbf{S}}\sin(\sqrt{\mathbf{S}}\,\Delta z/2) & \cos(\sqrt{\mathbf{S}}\,\Delta z/2)\end{pmatrix}\equiv\begin{pmatrix}\mathbf{P}_{11} & \mathbf{P}_{12}\\ \mathbf{P}_{21} & \mathbf{P}_{22}\end{pmatrix}. \quad (14)$$

Obviously, the matrix $\mathbf{P}^2$ is also a similar block matrix. Further, $\mathbf{Q}$ is also a block matrix as defined in Eq. (6) and its sub blocks include two unity matrices, a null matrix and a diagonal matrix. The first propagation step requires the evaluation of the following matrix products:

$$\mathbf{P\Phi}(z)=\begin{bmatrix}\mathbf{P}_{11}\boldsymbol{\psi}+\mathbf{P}_{12}\dfrac{\partial\boldsymbol{\psi}}{\partial z}\\ \mathbf{P}_{21}\boldsymbol{\psi}+\mathbf{P}_{22}\dfrac{\partial\boldsymbol{\psi}}{\partial z}\end{bmatrix}\equiv\begin{bmatrix}\boldsymbol{\xi}\\ \dfrac{d\boldsymbol{\xi}}{dz}\end{bmatrix} \quad (15)$$

and

$$\mathbf{Q}(z)\left\{\mathbf{P\Phi}(z)\right\}=\begin{bmatrix}\boldsymbol{\xi}\,\Delta z\\ -k_0^2\,\mathbf{R}(z)\dfrac{d\boldsymbol{\xi}}{dz}\Delta z\end{bmatrix} \quad (16)$$

The computation in Eq. (15) involves 8 multiplications of a $N_x\times N_x$ matrix by a column vector, since $\boldsymbol{\psi}$ is complex. Each of these operations uses N_x^2 multiplications. Thus the total

number of multiplications in the step represented by Eq. (15) is $8N_x^2$. This remains the same when one uses $\mathbf{P}^2$ instead of $\mathbf{P}$ in subsequent propagation steps. On the other hand, the evaluation of Eq. (16) involves multiplication of a diagonal matrix with a complex column vector, which uses only $2N_x$ multiplications. Further, two column vectors have to be multiplied by Δz. Thus, the total number of multiplications required in the evaluation of the step given in Eq. (16) is $6N_x$. Therefore, the first step, and each subsequent step, requires $(8N_x + 6)N_x$ multiplications. Since, generally the value of N_x is several hundred, one can approximate the number of multiplications in each step by $8N_x^2$. Thus the multiplications required to propagate N_z step would be nearly $8N_x^2 N_z$.

An estimation of the computational effort in evaluating the matrix $\mathbf{P}$ is not very simple as this evaluation involves the computation of sine, cosine and square root of a matrix. However, these operations are done on the matrix $\mathbf{S}$ and are, therefore, independent of the order, M, used in obtaining the matrix $\mathbf{S}$. On the other hand, the evaluation of the marix $\mathbf{S}$ up to order M requires M multiplications of $N_x \times N_x$ matrices and hence, the computation effort increases monotonically (almost linearly) as M increases. As an illustrative example, we have given in Fig. 1, the time, t_P, for one-time evaluation of the matrix $\mathbf{P}$, and the time, t_s, for propagating a single step as defined by Eqs. (15) and (16), as a function of order, M. These computations correspond to the waveguide and other parameters used in the example discussed in Sec. 3.1. The figure clearly shows that t_s is almost independent of M, whereas t_P increases with M. It also shows that t_P for $M = 1$ is equal to the time taken in propagating about 200 steps. The increase in t_P is of the same order for each increase of order by one, particularly for larger orders, $M > 10$, which are generally used (see the next section). Thus, the evaluation of the series in Eq. (12) is a major contributor to t_P. In our calculations, we have used MATLAB, and have made no effort in using the fact that the matrix $\mathbf{D}_x$ is sparse. This fact could be used to economize on matrix multiplications involved in evaluating the series in Eq. (12). One could also diagonalize the tri-diagonal matrix $\mathbf{D}_x$ and then evaluate the series. We are examining these and other possibilities to economize the evaluation of the matrix $\mathbf{P}$ to make overall propagation more efficient. The outcome of these investigations will be reported elsewhere.

3 Numerical Examples

In this section, we present results of some numerical examples to demonstrate the accuracy and stability of the method presented in the previous section, namely, the finite-difference based split-step non-paraxial (FD-SSNP) method. In our examples, we have considered three waveguides, which have been used in the literature for similar studies. The index profiles and other parameters of these waveguides are given in Table-I. Further, in our examples, we have considered the tilted waveguide geometry, which is depicted in Fig. 2. In all the examples, we launch at $z = 0$, a mode along the tilted waveguide so that we know exactly the field at the final distance, $z = z_f$. Then, we compare the numerically propagated field with the expected mode field at $z = z_f$; specifically we compute the correlation factor, *CF*:

$$CF = \frac{\left| \int \psi^*_{mode} \psi_{cal} \, dx \right|^2}{\left| \int |\psi_{mode}|^2 \, dx \right|^2} \tag{17}$$

where ψ_{mode} is the modal field launched at $z = 0$ and is also the expected field at $z = z_f$, and ψ_{cal} is the numerically propagated field at $z = z_f$. This definition of the correlation factor includes the effects of both the dissipation in power as well as the loss of shape of the propagating mode (Ilić et al., 1996). The error (*ERR*) in numerical propagation is given by

$$ERR = 1 - CF \tag{18}$$

and is a measure of the accuracy of the method used for numerical propagation.

In a tilted waveguide, the field $\psi_{mode}(x)$ at $z = 0$ would be the phase tilted modal field and would be given by

$$\psi_{mode}(x) = \psi_m(x) \exp(-i\beta_m x \sin\theta) \tag{19}$$

where θ is the tilt angle (see Fig. 2), and $\psi_m(x)$ and β_m are the modal field and the propagation constant of the mode launched. The exact modal fields at $z = 0$ and $z = z_f$ would differ by a constant phase factor, which would not alter the value of the *CF* and hence the same field $\psi_{mode}(x)$ is used for the input ($z = 0$) and the expected ($z = z_f$) fields in defining *CF*. Of course, the field at $z = z_f$ is shifted along the x-axis by a distance $z_f \tan\theta$.

In our examples, we have propagated the TE_0 mode in the graded-index waveguide (GRW) the modal field of which is defined as (Adams, 1981)

$$\psi_0(x) = \cosh^{-W}(2x/w) \tag{20}$$

where

$$W = \left(\beta_0^2 - 4\pi^2 n_s^2/\lambda^2\right)^{1/2} w/2 = \tfrac{1}{2}\left[(1+4V^2)^{1/2} - 1\right], \qquad V = \pi w (2n_s\Delta n)^{1/2}/\lambda . \quad (21)$$

In the examples with the step-index waveguides (SIW1 and SIW2), we have propagated the TE_1 and TE_{10} modes. The fields of these modes are well documented in several textbooks (see, e.g. Adams, 1981; Ghatak and Thyagrajan, 1998) and hence, are not repeated here.

3.1 Effect of Order, *M*

We first show the effect of the order M on propagation. As a test case we consider the propagation of the TE_0 mode in the graded-index waveguide (GRW) tilted at $\theta = 50^\circ$. Figure 3 shows the input field intensity and the expected and the numerically propagated field intensities after propagation up to $z_f = 100\mu\text{m}$; Δz used is 0.05 μm. Sub-figures (a) to (e) show these intensities for different orders, M and the sub-figure (f) shows *CF* as a function of order, M. From these results, we can see that for $M = 1$ (sub-figure a), the propagated field is distorted and does not get displaced in the transverse direction to the extent expected, and there is a large error in propagation. With an increase in order M, both the mode shape and mode displacement improve dramatically. The value of *CF* is nearly unity (up to 3 decimal places) for $M \geq 20$. This improvement in the accuracy is not accompanied by an increase in computation time for propagation, but only the time for one-time computation of the matrix $\mathbf{P}$ increases. This fact is illustrated by the computation times shown in Fig.1, which shows separately the time, t_P, required for the one time computation of $\mathbf{P}$ and the time, t_s required for propagation of a single step. The figure shows the actual time in seconds for the computations which have been done using MATLAB version 7 release 14 on a personal computer based on Intel Pentium 4, 3GHz processor with Windows XP Professional operating system.

3.2 Stability and Accuracy of Propagation

An important issue with all propagation methods is their stability. Figure 4 shows the stability performance of the present method with respect to propagation step-size for a large propagation distance (1000 μm) for the untilted graded-index waveguide. From the figure it can be seen, that even with a step-size as large as 1 μm, the method remains stable and the error is very low, of the order of 10^{-4}. To the best of our knowledge, a step-size as large as 1 μm has not been reported earlier for the finite-difference based wide-angle propagation method. We have earlier reported such a large step-size with the collocation based split-step non-paraxial (Coll SSNP) method (Sharma and Agrawal, 2004). Such a large step-size makes the computation faster and

more efficient. In the results of Shibayama *et al.* (1999), the largest step-size reported is $0.05\,\mu$m with a 3-step iterative process and 2000 points in a regular grid. This difference in the step-size itself makes the present method 20 times faster.

As another example to demonstrate the stability of the method, we consider the propagation of the TE_1 mode in a step-index waveguide, namely, the benchmark waveguide (SIW2). We have plotted in Fig. 5, *ERR* as a function of propagation distance for the untilted waveguide and for the waveguide tilted at an angle of 20^o. From the figure it is clear that even at 20^o the propagation is stable for a large distance, $500\,\mu$m and the error remains low, of the order of 10^{-2}-10^{-3}. This demonstrates the stability and the accuracy of the method. It may be pointed out that due to the relatively large index difference, we have taken a step-size of $0.05\,\mu$m, which corresponds to 10000 steps of propagation.

3.3 Comparison with Other Methods

Next, we consider examples to compare the performance of the present method, the FD-SSNP, with other methods. First we consider the propagation of the TE_0 mode in the graded index waveguide (GRW) as a function of the tilt angle. Figure 6 shows the variation of *ERR* with tilt angle of the waveguide for different propagation step-sizes for the finite difference (FD SSNP, solid line) and collocation (Coll SSNP, dashed line) implementations. The figure shows that the FD SSNP method is stable and accurate with a large step-size of $1.0\,\mu$m giving an accuracy of $\sim 10^{-2}$, while it gives accuracy of the order of 10^{-3} –10^{-4} with a step-size of $0.25\,\mu$m, which is much better than those obtained by Shibayama *et al.* (1999). To illustrate the point, let us consider the error for a tilt angle of 50^o. The error in the best results reported by Shibayama *et al.* (1999) for the 3-step GD scheme is about 0.04 with $\Delta z = 0.05\,\mu$m and 2000/1273 points regular/adaptive grid, whereas in our method (FD SSNP) the error is less than 0.001 with $\Delta z = 0.25\,\mu$m and only 900 grid points. This would thus mean much faster and more accurate propagation. From the figure we can also see that at lower angles for all step-sizes the Coll SSNP shows lower error, while at higher angles the performance of both the FD and the collocation implementations is similar or that of the FD implementation is better. This is expected as the collocation method involves interpolation over N_x points while FD implementation involves fewer points in the transverse domain. The important point is that even in the FD implementation, the present method performs much better than the Padé based method (Shibayama et al., 1999) and is faster and easier to implement. The added computational advantage is the flexibility to choose higher number of terms in the series

expansion for the transverse derivative for higher accuracy if required, and fewer terms if the accuracy requirement is not as stringent.

We next consider the propagation of the TE_1 mode of the step-index waveguide (SIW1). Figure 7 shows the variation in the error with the waveguide tilt angle for different propagation step-sizes for the Coll SSNP and FD SSNP for a propagation distance of 100 μm. We find that in the FD SSNP, with only $N_x = 900$ and Δz=0.25 μm, the value of *CF* at all angles from 0 to 50 degrees is about 0.995 or more which is significantly larger than ~0.92, the best value reported by Yamauchi *et al.* (1996) for the 3-step GD based method with a smaller step-size, 0.1 μm and 1800 computation points. In the FD SSNP, with a propagation step-size 2.5 times larger and only half the number of transverse grid points, the error in *CF* is smaller by an order of magnitude at 50^o. It may be noted that the present method is non-iterative unlike the method of Yamauchi *et al.* (1996), which is a 3-step iterative process. In this example, both the FD SSNP and Coll SSNP show similar errors and over all one can conclude that both perform equally well.

Table II shows the performance of the method for the TE_1 mode in the benchmark waveguide (SIW2). As the refractive index change from core to cladding is very large in this case, the propagation step-size is smaller than for the step index waveguide in the example given above. In the FD SSNP, we have used $N_x = 1200$, $\Delta z = 0.05\mu$m and *M*=60. At 40^o waveguide tilt angle, the error in propagation is similar to that obtained by Yamauchi *et al.* (1996) with $N_x = 1800$ points and a 3-step GD based method. However, our method is computationally more efficient. Comparing the Coll SSNP and FD SSNP, we can see that the former is more accurate at lower angles, while the latter is better at larger angles.

The final example is that of the propagation of the TE_{10} mode in the benchmark waveguide (SIW2) and we have obtained the power remaining in the guide after propagation over 100 μm at a tilt angle of 20^o. Table III compares the two SSNP methods with other methods reported by Nolting and März (1995). It is evident from the table that with smaller N_x, the SSNP methods show significantly higher accuracy. The FD SSNP is more accurate than the Coll SSNP. This is probably because the former performs equally well or better than the latter at larger angles. It may further be noted that in the Coll SSNP, the error does not decrease much on increasing the number of steps from 1000 to 2000 (by halving Δz); it changes only in the third decimal place.

An important parameter to choose is the reference refractive index, n_r. Although, in principle, its value can be arbitrarily chosen, its value may in general affect the accuracy. Figure 8 shows the *ERR* as a function of n_r for the Coll SSNP and the FD SSNP. These results show that the accuracy is largely insensitive to the choice of n_r for both these methods.

4 Conclusions

A finite difference solution of the second order wave equation implemented in the split step scheme has been presented. The formulation is non-iterative and allows arbitrary increase in accuracy in approximating the transverse derivatives, without any significant increase in computation. The method involves only simple matrix multiplication for propagation, and is stable with larger step-sizes than reported in other existing methods. The method has excellent efficiency in terms of increased accuracy, lower computation effort and easier implementation.

Comparison with other methods show that this method gives much better accuracy and involves less computational effort in comparison to the generalized Douglas (GD) and Padé approximants based finite-difference methods. However, in comparison to the previously reported collocation based split-step non-paraxial method, the present method gives better performance for larger tilt angles (typically more than 20^o), while the for smaller angles the collocation method performs better.

Acknowledgements

This work was partially supported by a grant (No. 03(0976)/02/EMR-II) from the Council of Scientific and Industrial Research (CSIR), India. One the authors (AS) is a Senior Associate Member of the Abdus Salam International Centre for Theoretical Physics, Trieste, Italy and the other author (AA) would like to thank the Centre for hospitality and support during her visit to the Centre.

References

Adams, M. J., *An Introduction to Optical Waveguides*, New York, John Wiley, 1981.

Conte, S.D., and C. deBoor, Elementary Numerical Analysis, New York, McGraw-Hill (1972).

Ghatak, A.K. and K. Thyagarajan, *Introduction to Fiber Optics*, Cambridge, University Press, 1998.

Hadley, G.R., Opt. Lett. **17** 1743, 1992.

Ho, P.L. and Y.Y.Lu, IEEE Photon. Technol. Lett. **13** 1316, 2001.

Ilić, I., R. Scarmozzino and R. Osgood, J. Lightwave Technol., **14** 2813, 1996.

Khabaza, M., Numerical Analysis, London, U.K, Pergamon Press, pp. 55-58, 1965.

Lu, Y.Y. and P.L.Ho, Opt. Lett. **27** 683, 2002.

Lu, Y.Y. and S.H. Wei, IEEE Photon. Technol. Lett. **14** 1533, 2002.

Luo, Q. and C.T. Law, IEEE Photon. Technol. Lett. **14** 50, 2002.

Nolting, H.-P. and R. März, J. Lightwave Technol. **13** 216, 1995.

Sharma, A. and A. Agrawal, J. Opt. Soc. Am. A **21** 1082, 2004.

Sharma, A. and A. Agrawal, European Conference on Integrated Optics, Grenoble, France, April 5-8, 2005.

Sharma, A. and A. Agrawal, IEEE Photon. Technol. Lett. (In press, 2006).

Sharma A. and S. Banerjee, J. Opt. Soc. Am. A **6**, 1884, 1989; *Errata*: **7**, 2156, 1990.

Sharma, A., In: Methods for Modeling and Simulation of Guided-Wave Optoelectronic Devices, W.P. Huang, Ed. Cambridge, Massachussettes: EMW Publishers, pp. 143-198, 1995.

Shibayama, J., K. Matsubara, M. Sekiguchi, J. Yamauchi and H. Nakano, J. Lightwave Technol. **17** 677, 1999.

Sun L. and G. L. Yip, Opt. Lett. **18** 1229, 1993.

Yamauchi, J., J. Shibayama, M. Sekiguchi and H. Nakano, IEEE Photon. Technol. Lett. **8** 1361, 1996.

Yevick, D. and M. Glasner, Opt. Lett. **15** 174, 1990.

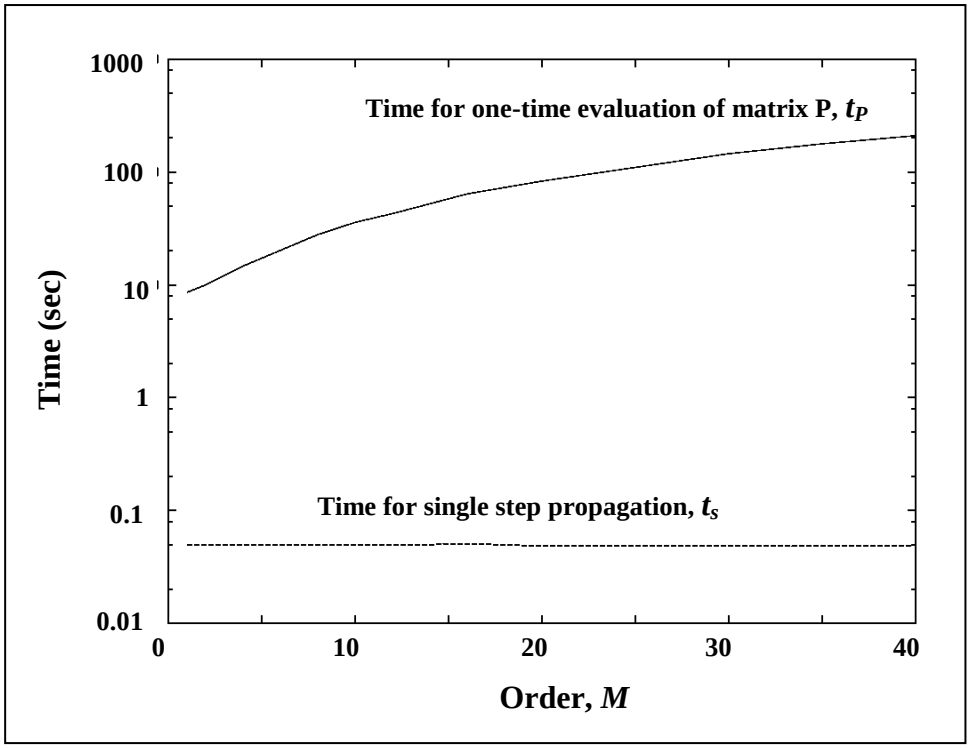

Figure 1 Computation time for the one-time evaluation of the matrix **P** and for single step propagation as a function of the order M for the graded-index waveguide (GRW) for the details of the waveguide see Table-I and for other details see Sec 3.1.

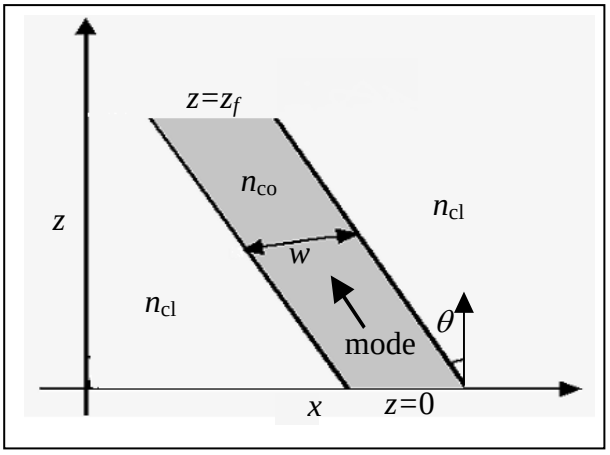

Fig. 2 Geometry of the tilted waveguide

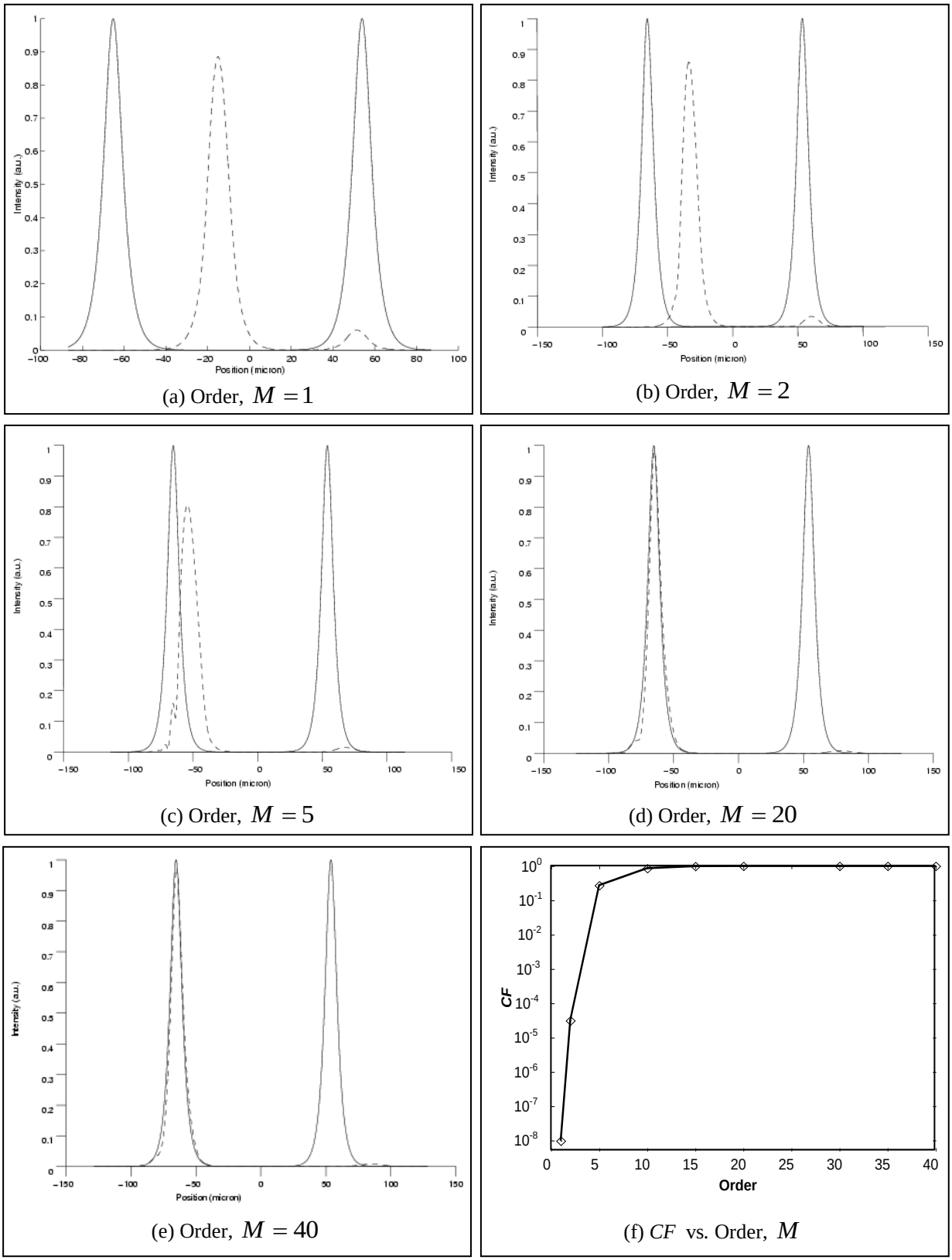

(a) Order, $M = 1$

(b) Order, $M = 2$

(c) Order, $M = 5$

(d) Order, $M = 20$

(e) Order, $M = 40$

(f) *CF* vs. Order, M

Figure 3 (a-e) Plots of the TE_0 mode propagated in the graded-index waveguide (GRW) for 100 μm at 50^0 with different orders, *M*. The input field (rightmost curve), propagated field (dashed curve) and the expected field (leftmost curve) are shown. **(f)** Variation of the correlation factor (*CF*) as a function if the order *M*.

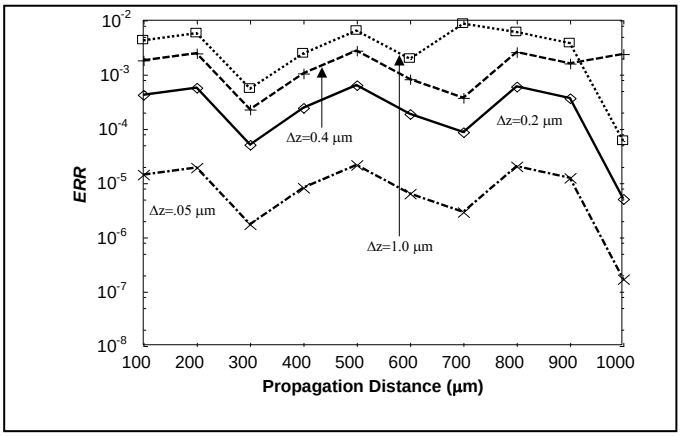

Figure 4 *ERR* as a function of propagation distance for the graded-index waveguide (GRW). *N*=900, order=35.

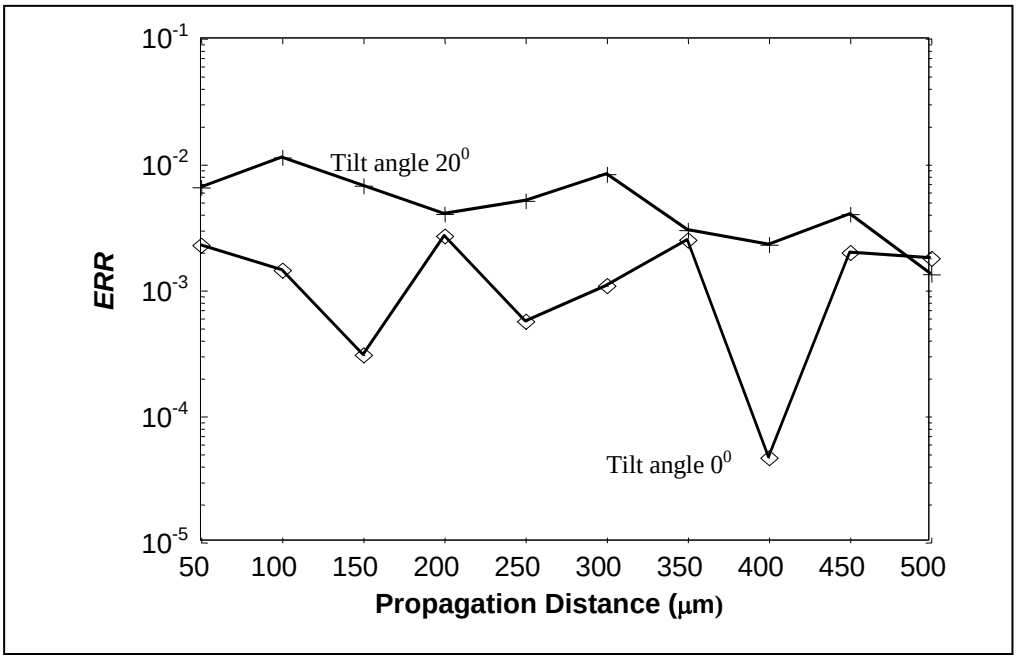

Figure 5 *ERR* as a function of propagation distance for the step-index waveguide (SIW2) (Nolting and März , 1995). *N*=1200, order=60.

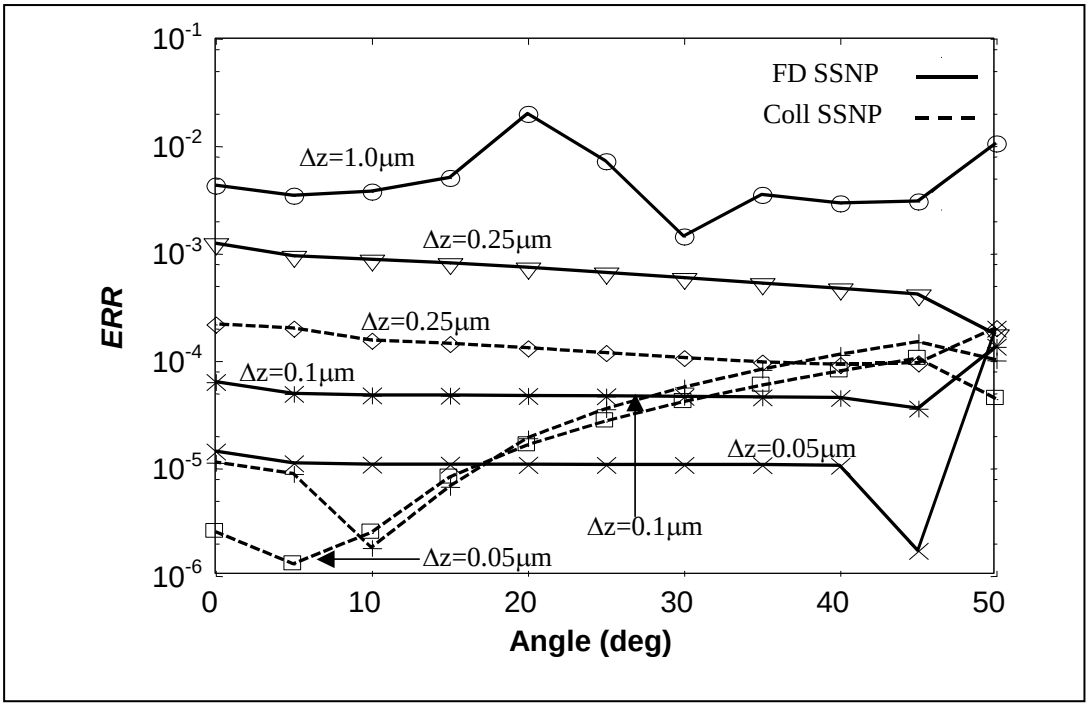

Figure 6 *ERR* as a function of waveguide tilt angle for the graded-index waveguide (GRW) (Shibayama *et al*., 1999) of length 100 μm . For the FD SSNP: *N*=900, order=35.

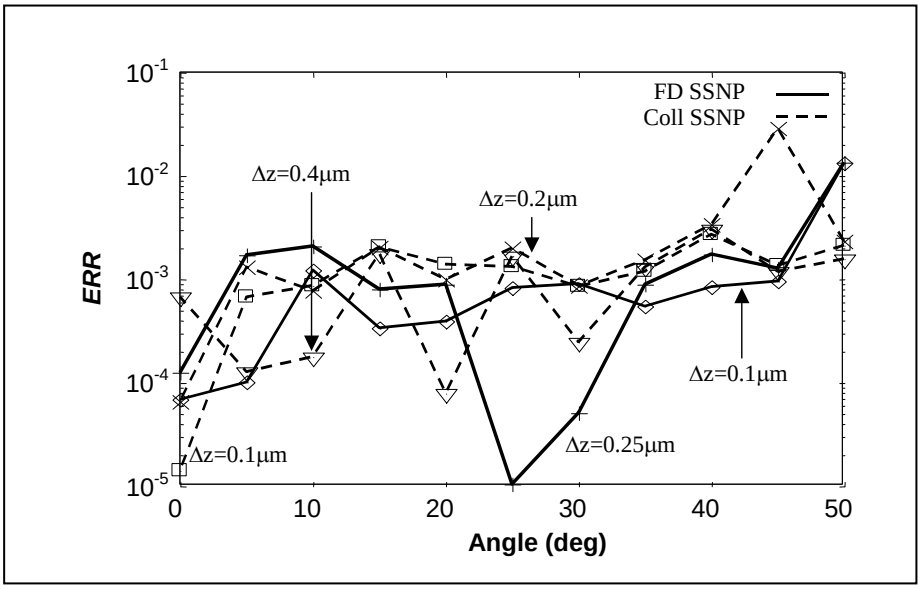

Figure 7 *ERR* as a function of waveguide tilt angle for the step-index waveguide (SIW1) (Yamauchi *et al.* 1996). .For the FD SSNP: *N*=900, order=30.

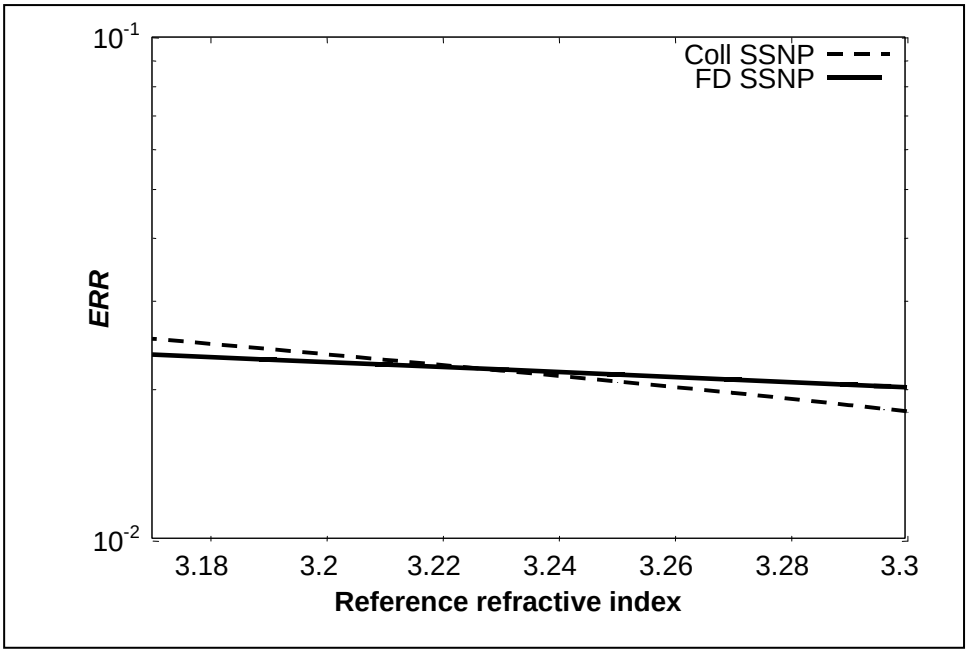

Figure 8 Error in propagation with the reference refractive index for the benchmark step-index waveguide (SIW1) for propagation up to 100 μm with step size 0.1 μm at 40°.

Table-I: Waveguide Profiles and Parameters

Waveguide		**Profile and Parameters**
GRW	Graded-index waveguide (Shibayama et al., 1999)	$n^2(x) = n_s^2 + 2n_s\Delta n \operatorname{sech}^2(2x/w)$ n_s=2.1455, Δn=0.003, w=5μm, λ=1.3 μm
SIW1	Step index waveguide (Yamauchi et al., 1996)	n_{co}=1.002, n_{cl}=1.000, w=15.092 μm, λ=1.0 μm
SIW2	Step index waveguide (benchmark waveguide) (Nolting and März, 1995)	n_{co}=3.30, n_{cl}=3.17, w=8.8 μm,λ=1.55 μm

Table-II: *ERR* at different angles for the TE_1 mode in the benchmark waveguide (SIW2) for 100 μm propagation. Results for Coll SSNP and FD SSNP implementation are presented.

Angle (degrees**)**	***ERR***	
	FD SSNP	**Coll SSNP**
0	1.06×10^{-4}	2.82×10^{-5}
10	8.0×10^{-3}	6.80×10^{-3}
20	4.64×10^{-3}	9.95×10^{-3}
30	4.14×10^{-3}	8.00×10^{-3}
40	2.02×10^{-2}	3.60×10^{-2}
50	2.66×10^{-2}	2.24×10^{-2}

Table-III: Power remaining in the waveguide after propagation through 100 μm in the benchmark waveguide (SIW2) for TE_{10} modes using different methods.

Method	N_z	N_x	Power in waveguide at 20^o
FD SSNP	2000	320	~0.99
Coll SSNP	2000	800	~0.96
Coll SSNP	1000	800	~0.96
AMIGO*	1429	1311	~0.95
FD2BPM*	1000	2048	~0.95
FTBPM*	1000	256	~0.55
LETI-FD*	200	1024	~0.15

* Results taken from Nolting and März (1995).